Precision test of the rotor model from band mixing in ^{166}Er

W. D. Kulp, J. M. Allmond, P. Hatcher, and J. L. Wood
School of Physics, Georgia Institute of Technology, Atlanta, Georgia 30332-0430, USA

J. Loats,* P. Schmelzenbach,† C. J. Stapels,‡ and K. S. Krane
Department of Physics, Oregon State University, Corvallis, Oregon 97331-6507, USA

R.-M. Larimer§ and E. B. Norman||
Nuclear Science Division, Lawrence Berkeley National Laboratory, Berkeley, California 94720, USA
(Received 24 August 2005; published 24 January 2006)

The relative γ-ray intensities for the γ-to-ground interband transitions and the γ band $\Delta I = 2$ intraband transitions in ^{166}Er have been measured with high precision. These intensities have been used to generate interband relative $B(E2)$'s. The results are presented in a Mikhailov plot and are consistent with a cubic polynomial fit at the 0.60% precision level. The significance of the fit is discussed.

DOI: 10.1103/PhysRevC.73.014308 PACS number(s): 21.60.Ev, 27.70.+q

I. INTRODUCTION

The rotor model applied to deformed nuclei has been enormously successful since its introduction by A. Bohr [1]. For the most strongly deformed nuclei it describes excitation energies and electric quadrupole properties very well in zeroth order. The first-order corrections to rotational energies [the $I^2(I+1)^2$ term], in the best cases, achieve descriptions accurate to, for example, $\pm 1\%$ at $I = 10$. Precision tests of electric quadrupole properties, $E2$ transitions and quadrupole moments, have been lacking because of the experimental difficulty associated with measuring the quantities accurately. For example, the most precisely measured $B(E2; 6^+ \rightarrow 4^+)$ values in ground-state bands of doubly even nuclei have uncertainties of $\pm 2\%$, and the most precisely known $Q(6^+)$ values in such bands have uncertainties of $\pm 5\%$. There are indications [2] that within the ground-state bands of strongly deformed doubly even nuclei the $B(E2)$ values are consistent with the rotor model to zeroth order.

A way to carry out precision tests of the electromagnetic properties of the rotor model is to use $E2$ transition branching ratios between bands, albeit at the expense of involving two rotational bands instead of one. Such an approach circumvents the limitations on the precision of lifetime measurements for rotational states. The theory of rotational band mixing and the quantification of interband $E2$ transition strengths was elucidated [3–6] in the early days of the nuclear rotor model. Since its inception, band mixing has received sustained recognition, especially in its application to the description of transition strengths between the ground-state ($K^\pi = 0^+$) band and the lowest $K^\pi = 2^+$ ("gamma") band in doubly even nuclei, with the focus primarily on failures of simple mixing descriptions (see, e.g. [6–8]). Failures appear to be due to mixing with a third band. Thus, the best cases for precision tests appear to be where the γ band is well removed in energy from other excited (positive-parity) bands.

The best-studied example of ground γ-band mixing is in ^{166}Er. This nucleus was chosen as a case study in the monograph by Bohr and Mottelson [9]. Besides the relative isolation (in energy) of the γ band, the nucleus ^{166}Er offers unique experimental advantages: The γ band is populated in the radioactive decays of ^{166}Tm ($I^\pi = 2^+$, $T_{1/2} = 7.70$ h) and ^{166m}Ho ($I^\pi = 7^-$, $T_{1/2} = 1200$ yr), which can yield precise relative γ-ray intensities (and hence precise relative $E2$ transition probabilities) up to $I = 8$ and a total of 17 interband transitions in all. These transitions and the corresponding ground-band and γ-band levels are shown in Fig. 1.

Many of the transitions of interest for a band-mixing study are relatively well known because the decay of ^{166m}Ho to ^{166}Er has been the subject of numerous experimental studies. Some of these studies have focused on issues of structure [11–13] and have explicitly addressed Mikhailov band mixing, and some have been concerned precision γ-ray relative intensity measurements in pursuit of developing ^{166m}Ho as a secondary standard for detector photopeak efficiency calibration [14]. This latter aspect proves invaluable for a test of band mixing because the standardized lines provide a precise set of intensities for relative photopeak efficiency calibration of the detector system.

The major ^{166m}Ho β-decay branches [10] with subsequent feeding of the γ band are to 6^- states at 1787.0 keV (76.4%) and 1827.6 keV (17.7%), both of which decay predominantly to the 5_γ, 6_γ, and 7_γ states. Although there are also minor β-decay branches (intensities <3%) [10] directly to the $J = 6, 7, 8$ states of the γ band and the $J = 6, 8$ states in the ground-state band, there is only weak subsequent decay to the

*Present address: Department of Physics and Engineering, Fort Lewis College, Durango, Colorado 81301, USA.
†Present address: Department of Chemistry and Physics, Erskine College, Due West, South Carolina 29639, USA.
‡Present address: Radiation Monitoring Devices, 44 Hunt Street, Watertown, Massachusetts 02472, USA.
§Deceased
||Present address: L-414, Lawrence Livermore National Laboratory, P.O. Box 808, Livermore, California 94551, USA.

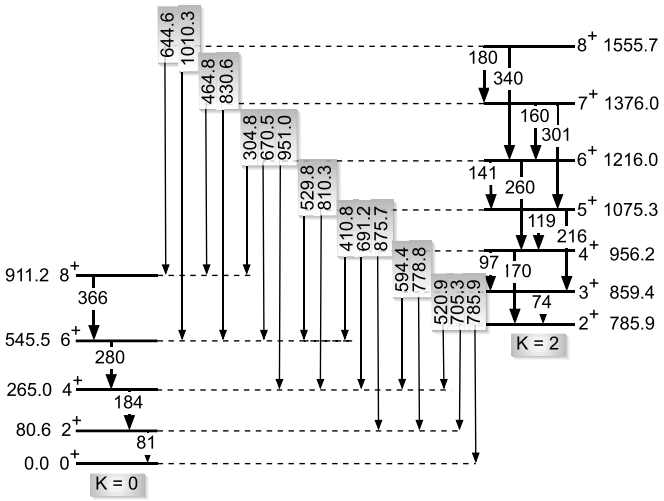

FIG. 1. Levels and transitions in the ^{166}Er ground and γ bands relevant to the present study labeled by energy in keV. The data are from Nuclear Data Sheets for $A = 166$ [10].

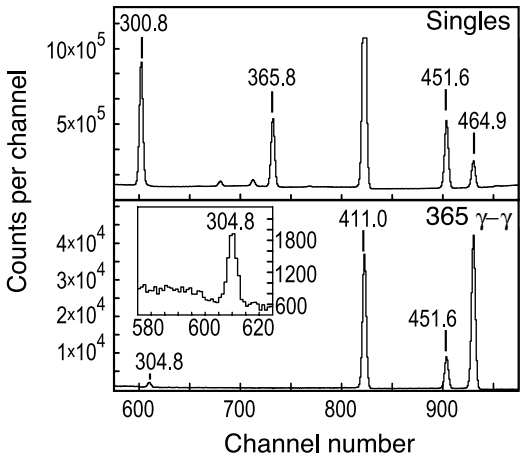

FIG. 2. In the ^{166m}Ho decay singles spectrum, the 300.8-keV γ ray obscures the region near ~300 keV. A coincidence gate on the $8_g \rightarrow 6_g$ (366-keV) line reveals the very weak 304.8-keV line ($6_\gamma \rightarrow 8_g$, cf. Fig. 1).

2_γ state. (The strongest γ ray out of this level, the 705.32 keV $2_\gamma \rightarrow 2_g$ transition, has an intensity of $I_\gamma = 0.025$ [10].) In contrast, the 2_γ, 3_γ, 4_γ, and 5_γ states are fed via 3^+ states at 2132.9 and 2160.1 keV in ^{166}Er, which are strongly populated in the decay of ^{166}Tm. The decay of ^{166}Tm to ^{166}Er has been the subject of only a few experimental studies [15–17], and the uncertainty on the adopted [10] intensity for the $2_\gamma \rightarrow 4_g$ transition is greater than 10%.

Three main challenges must be met for the precision data required to test the rotor model using Mikhailov band mixing in ^{166}Er. First, a number of pertinent transitions, for example, $I_\gamma(304.8\,\text{keV}) = 0.0228/100$ ^{166m}Ho β decays, are populated very weakly. Second, the 410.8/410.9- and the 520.9/521.0-keV doublets in the ^{166m}Ho and ^{166}Tm decay schemes, respectively, obscure γ rays of interest (cf. Fig. 1). Third, some lines are distorted by close-lying sum peaks or by severe nonlinearities in the underlying Compton continuum. High-statistics coincidence data with attention to summing and angular correlation effects are required to confront these problems.

II. EXPERIMENTS

Gamma-ray spectroscopy following the β decay of ^{166m}Ho and ^{166}Tm was carried out at the Lawrence Berkeley National Laboratory 88-Inch Cyclotron using the 8π spectrometer [18]. This is an array of 20 Compton-suppressed Ge detectors with (nominal) characteristics as follows: Volume = 115 cm^3, diameter = 51.5 mm, resolution = 3.0 keV FWHM at 1332 keV, and peak:total = 0.48 at 677 keV. The array was configured with source-to-detector distances of 22.0 cm and detectors were pairwise distributed at angles of 41.8°(60), 70.5°(120), 109.5°(120), 138.2°(60), and 180.0°(20). Pairwise angle combinations result in low angular correlation distortions (e.g., 0.57% and 1.50% attenuations for 4–2–0 and 2–4–2 spin cascades, respectively) for coincidence intensities.

The ^{166m}Ho source (5 ml solution of $HoCl_3$ dissolved in 0.1 *M* HCl) was obtained from Isotope Products Laboratories (Burbank, CA). This source contained $(4.7 \pm 0.2)\%$ ^{154}Eu, determined as a disintegration rate in this study, and had a strength of ~9μCi. A 3.8-cm-tall, 1.0-cm-diameter glass vial inside of a 5.1-cm-tall, 1.6-cm-diameter polyethylene screw-top sample cylinder held the liquid during the measurement.

A total of 1.5×10^8 $\gamma\gamma$ coincidence events were recorded in a running time of 107 h in the ^{166m}Ho decay study. The quality of the data is illustrated in Fig. 2, which shows a region of the γ-ray singles spectrum compared with the same region gated by the $8_g \rightarrow 6_g$ (366-keV) transition. The very weak 304.8-keV line ($6_\gamma \rightarrow 8_g$ transition) is evident only in the coincidence spectrum. We determine an intensity for this γ ray of $0.0228 \pm 0.0008/100$ β's, which can be compared with 0.022 ± 0.002 [10] and 0.016 ± 0.001 [14].

The ^{166}Tm sources were produced via the decay of ^{166}Yb ($T_{1/2} = 56.7$ h), made using the ^{166}Er(α,4n) reaction by bombarding 96.3% enriched $^{166}Er_2O_3$ powder with a 50-MeV ^{4}He beam from the 88-Inch Cyclotron. The oxide powder was dissolved in HNO_3 and the resulting solution was packaged similarly to the ^{166m}Ho source for measurement in the 8π spectrometer; typical source strengths were ~25μCi. Source impurities included ^{167}Tm and ^{165,168}Tm (traces).

In the ^{166}Tm decay study, 2.9×10^8 $\gamma\gamma$ coincidence events were recorded in a running time of 266 h. Figure 3 shows the sensitivity for determining the intensity of the $2_\gamma \rightarrow 4_g$ (521-keV) transition using coincidence gating by the 1374-keV ($2160 \rightarrow 2_\gamma$) transition. The Compton continuum under the 521-keV peak (nonlinearity from the 706-keV γ ray) was fitted using the nonlinear profile of the Compton "bump" from the 786-keV γ ray (shifted to account for the γ-ray energy dependence of this feature).

III. DATA ANALYSIS AND RESULTS

The relative γ-ray intensities for strong lines (184, 280, 366, 530, 594, 670, 691, 779, 810, 831, 951, 1147, 1241, 1401,

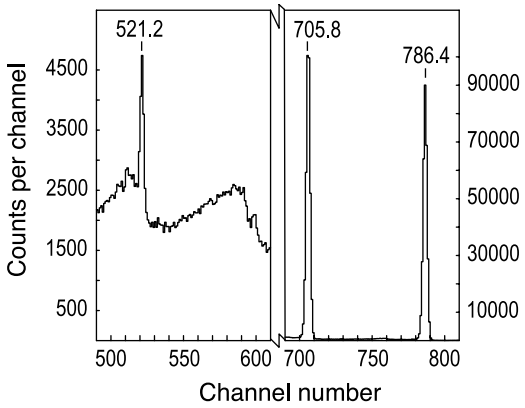

FIG. 3. γ-ray transitions $2_\gamma \rightarrow 4_g, 2_g, 0_g$ observed in coincidence with the $2160 \rightarrow 2_\gamma$ transition in the decay of ^{166}Tm. Energies are given in keV. The $2_\gamma \rightarrow 4_g$ transition at 521.2-keV is discussed in the text.

and 1427 keV) associated with the β decay of ^{166m}Ho were used to calibrate the relative photopeak efficiency response of the array. Further, these calibration lines also provided a number of precise relative γ-ray intensities for input to the determination of relative $E2$ transition probabilities. Table I lists the transitions used in the band-mixing calculations and

TABLE I. γ ray transitions relevant to the present study and the intensities adopted.

Transition	Energy[a] (keV)	Intensity[b]	$\Delta I(\%)$	Source[c]
$8_\gamma \rightarrow 8_g$	644.61	0.2097	1.38	Ho
$8_\gamma \rightarrow 6_g$	1010.29	0.1096	1.75	Ho
$8_\gamma \rightarrow 6_\gamma$	339.74	0.226	1.55	Ho
$7_\gamma \rightarrow 8_g$	464.80	1.639	1.15	Ho
$7_\gamma \rightarrow 6_g$	830.58	13.52	0.52	NDS
$7_\gamma \rightarrow 5_\gamma$	300.76	5.14	0.58	NDS
$6_\gamma \rightarrow 8_g$	304.82	0.0314	3.71	Ho
$6_\gamma \rightarrow 6_g$	670.50	7.55	0.53	NDS
$6_\gamma \rightarrow 4_g$	950.97	3.795	0.32	NDS
$6_\gamma \rightarrow 4_\gamma$	259.74	1.446	1.17	Ho
$5_\gamma \rightarrow 6_g$	529.80	13.35	0.67	NDS
$5_\gamma \rightarrow 4_g$	810.28	80.0	0.38	NDS
$5_\gamma \rightarrow 3_\gamma$	215.89	3.59	1.95	NDS
$4_\gamma \rightarrow 6_g$	410.80	0.0233	2.23	Tm[d]
$4_\gamma \rightarrow 4_g$	691.25	1.85	1.08	NDS
$4_\gamma \rightarrow 2_g$	875.65	1.026	1.59	(Ho,Tm[d])[e]
$4_\gamma \rightarrow 2_\gamma$	170.31	0.0197	2.91	Ho
$3_\gamma \rightarrow 4_g$	594.43	0.775	1.16	NDS
$3_\gamma \rightarrow 2_g$	778.82	4.24	0.71	NDS
$2_\gamma \rightarrow 4_g$	520.95	0.0172	2.07	Tm
$2_\gamma \rightarrow 2_g$	705.32	1.000		Tm
$2_\gamma \rightarrow 0_g$	785.89	0.9059	1.05	Tm

[a]Calculated from differences of adopted [10] level energies.
[b]Normalized (^{166m}Ho decay) to $I_\gamma(810.28) \equiv 80.0$ ($\equiv 58.1/100$ β decays, i.e., $\times 0.726$ [10]) or (^{166}Tm decay) $I_\gamma(705.32) \equiv 1.000$.
[c]NDS(I_γ taken from NDS adopted value [10]); Ho (I_γ extracted from the ^{166m}Ho data; Tm (I_γ extracted from the ^{166}Tm data).
[d]Normalized through $I_\gamma(691.25) \equiv 1.85$ (^{166m}Ho decay).
[e]Average of Ho and Tm.

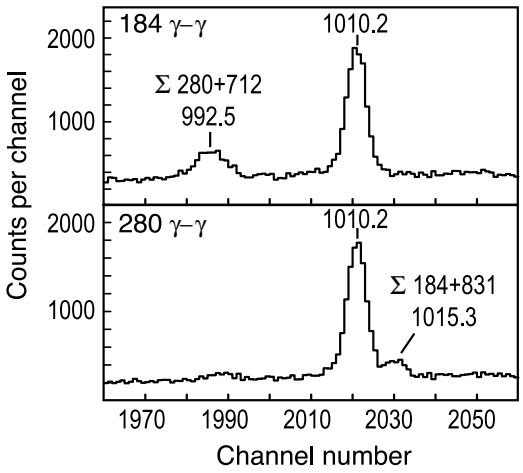

FIG. 4. The 1010.2-keV ($8_\gamma \rightarrow 6_g$) γ ray is unobscured in the 184-keV ($4_g \rightarrow 2_g$) gate. Measurement of the 1010.2-keV line in the 280-keV ($6_g \rightarrow 4_g$) gate is hindered by the sum peak at 1015.3 keV.

notes whether intensities were taken from the ^{166m}Ho evaluated decay data [10] or were obtained in the measurements reported here.

We have carried out a detailed summing analysis for our ^{166m}Ho decay data. In the case of the $8_\gamma \rightarrow 6_g$ (1010-keV) transition, shown in Fig. 4, the direct $6_g \rightarrow 4_g$ (280-keV) gated spectrum contains a sum peak at 1015 keV (Σ 184 + 831), which partially obscures the 1010-keV line and limits the measurement precision. However, the 1010-keV line is unobscured in the $4_g \rightarrow 2_g$ (184-keV) gate (also shown in Fig. 4), and we determine an intensity of $0.0796 \pm 0.0014/100$ β's using this gate (cf. $I_\gamma(1010\,\text{keV}) = 0.077 \pm 0.002$ [10] and $I_\gamma(1010\,\text{keV}) = 0.073 \pm 0.003$ [14]). Typical summing losses were determined to be 0.50%, approximately one-fifth those observed by Gehrke *et al.* [19] (whose source-to-detector distance was 15 cm versus 22.0 cm for ours). The largest summing gain for lines of interest to the present study was for the $6_\gamma \rightarrow 4_g$, 951.0-keV transition ($\Sigma 670.5 + 280.4$), which amounted to 0.24%. Summing effects for the ^{166}Tm $\rightarrow$ ^{166}Er decay scheme were similarly at a level too low to impact the precision of the present study.

Possible corrections for $M1$ admixtures in the $\Delta I = 0, 1$ transitions must be considered in the conversion of the relative γ-ray intensities in Table I into relative $B(E2)$'s. We have adopted the $\delta(E2/M1)$ mixing ratios of Hamilton *et al.* [20] for all the $\Delta I = 1, 0$ transitions except the $2_\gamma \rightarrow 2_g$ transition, which has been determined [21] to be $-(0.008 \pm 0.015)$. These have been converted into percentage $E2$ components, which are uniformly $\geqslant$99.7% except for the $8_\gamma \rightarrow 8_g$ transition, which is $96.0^{+2.1}_{-2.5}$%.

IV. BAND-MIXING ANALYSIS

We depict the results of the present study in the standard "Mikhailov plot" form in Fig. 5. This was established using the procedure adopted by Bohr and Mottelson [9]. The absolute magnitude is set from $\langle 2_\gamma | M(E2) | 0_g \rangle$: We adopt the value 0.373 ± 0.009 e b from data presented in Table II.

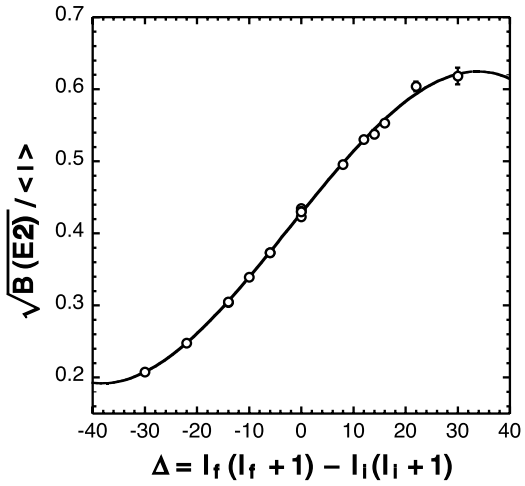

FIG. 5. Plot of our results in terms of the relationship given in Eq. (2) (Mikhailov plot) and our least-squares-fitted cubic polynomial. The experimental data are open circles. Error bars reflecting ΔI_γ (cf. Table I) are given where they exceed the size of circles. Note that there are two points at $\Delta = -14$, two points at $\Delta = -6$ (one fitted: see text), and four points at $\Delta = 0$.

Relative intensities for the $2_\gamma \to 0_g$, $2_\gamma \to 2_g$, and $2_\gamma \to 4_g$ then set the magnitude of the plot's initial slope and $\Delta = 0$ intercept. The two points associated with decay of the 3_γ level were fixed by normalizing the $3_\gamma \to 4_g$ ($\Delta = -6$) point to the $2_\gamma \to 0_g$ ($\Delta = -6$) point. The 12 points involving decays from the 8_γ, 7_γ, 6_γ, 5_γ, and 4_γ levels were set by establishing the value of Q_0^γ that optimally fits all these points to the initially established slope and $\Delta = 0$ intercept. This was done using the intensities of the $8_\gamma \to 6_\gamma$ transition relative to the $8_\gamma \to 8_g$ transition, etc. The fitted value of Q_0^γ is 8.028 e b, which can be compared with $Q_0^g = 7.656 \pm 0.033$ e b [31]. The relationship between Q_0^γ and the intraband $B(E2)$'s for a rigid rotor is

$$B(E2; I, K = 2 \to I - 2, K = 2) = \frac{5}{16\pi}\frac{3(I-2)(I-3)(I+2)(I+1)}{(2I-2)(2I-1)I(2I+1)}\left(Q_0^\gamma\right)^2. \quad (1)$$

TABLE II. Experimental values for $\langle 2_\gamma | M(E2) | 0_g \rangle$ and the (linearly weighted) average adopted in the present study. Processes are listed by light-ion inelastic scattering, heavy-ion Coulomb excitation (Coul. Ex.), and Coulomb excitation paired with the Recoil Distance Method (Coul. Ex.-RDM).

Process	$\langle 2_\gamma \lvert M(E2) \rvert 0_g \rangle e$ b	Source
Coul. Ex.	0.372 (19)	[22]
Coul. Ex.-RDM	0.331 (17)	[23]
$(p,\ p')$	0.360 (7)	[24]
$(\alpha,\ \alpha'\gamma)$	0.374 (11)	[25]
$(\alpha,\ \alpha')$	0.420 (10)	[26]
$(\alpha,\ \alpha')$	0.374 (8)	[27]
$(\alpha,\ \alpha')$	0.377 (7)	[28]
Coulomb	0.366 (12)	[29]
$(d,\ d')$	0.390 (10)	[30]
Average	0.373 (9)	

The plotted quantities and their uncertainties are given in Table III. The uncertainty of 2.4% in $\langle 2_\gamma | M(E2) | 0_g \rangle$ (cf. Table II) is not incorporated into any of the uncertainties given in Table III. This uncertainty would raise or lower the entire plot shown in Fig. 5; but it would not change the shape of the plot.

The plot shown in Fig. 5 can be fitted by the cubic relation (here, $m_0 = M_1/\sqrt{2}, m_1 = M_2/\sqrt{2}, m_2 = M_3/\sqrt{2}, \ldots$, cf. [9])

$$\frac{\sqrt{B(E2;\ I_i \to I_f)}}{\langle I_i 22 - 2 | I_f 0 \rangle} = m_0 + m_1\Delta + m_2\Delta^2 + m_3\Delta^3, \quad (2)$$

where $\Delta \equiv [I_f(I_f+1) - I_i(I_i+1)]$, $m_0 = 0.427666\, e$ b, $m_1 = 8.98016 \times 10^{-3} e$ b, $m_2 = -1.51023 \times 10^{-5} e$ b, and $m_3 = -2.31703 \times 10^{-6} e$ b. The R^2 for the fit is 0.998821. The deviations of the fit from the data, given in Table III, can be compared with the uncertainties in ΔI_γ, given in Table I, by dividing ΔI_γ by 2 (for the square-root dependence of the data points with respect to I_γ). The fit lies within 1σ for nine points and within 2σ for all but two points. We note the role of the 304.8- and 1010.3-keV transitions (cf. Figs. 2 and 4), respectively the $\Delta = +30$ and $\Delta = -30$ points in Fig. 5, which are key in establishing the cubic term. The difficulty of precisely determining the intensities of these very weak γ rays is the reason that the cubic term has not been observed previously.

Using a perturbation theory approach [9], it is possible to estimate the magnitudes of the quadratic (m_2) and cubic (m_3) terms in Eq. (2). However, as pointed out by Bohr and Mottelson (see their Eq. (4–235), p. 161 [9]), if $Q_0^\gamma \neq Q_0^g$ then there are additional contributions. We have estimated the magnitude of the quadratic term, which has contributions proportional to m_1^2/m_0 and $m_1(Q_0^g - Q_0^\gamma)/m_0$, where we use the m_0, m_1, Q_0^g, and Q_0^γ values given here. We obtain $m_2 \sim -3 \times 10^{-5}\, e$ b, which is of the correct order of magnitude [cf., $m_2(\text{fitted}) = -1.5 \times 10^{-5}\, e$ b] and sign. This reveals that the value $m_3/m_2 \cong 0.15$, obtained in the fit, is larger than can be explained by continuing the perturbation expansion.

To investigate the large cubic term in the Mikhailov plot for ^{166}Er we have also studied the $E2$ properties of the ground and γ bands using $\Delta K = 2$ two-band mixing. We used the Hamiltonian

$$H(I) = \begin{pmatrix} AI(I+1) & G\sqrt{2I(I+1)(I-1)(I+2)} \\ G\sqrt{2I(I+1)(I-1)(I+2)} & AI(I+1) + 4F \end{pmatrix} \quad (3)$$

and the $E2$ transition operator

$$\hat{T}^{(2)} = e\sqrt{\frac{5}{16\pi}}\left[\hat{T}_0^{(2)}\cos\gamma + \frac{1}{\sqrt{2}}\left(\hat{T}_{+2}^{(2)} + \hat{T}_{-2}^{(2)}\right)\sin\gamma\right], \quad (4)$$

which are adapted from [32]. The diagonal energy parameters are given by

$$A = \tfrac{1}{6}E(2_g), \quad (5)$$

$$F = \tfrac{1}{4}[E(2_\gamma) - E(2_g)]; \quad (6)$$

TABLE III. Transitions relevant to the present study and the $\sqrt{B(E2;\ I_i \to I_f)}/\langle I_i 22 - 2|I_f 0\rangle \equiv \sqrt{B_{\rm norm}(E2)}/\langle|\rangle\ e\,{\rm b}$ adopted.

Transition	Δ	$\langle\|\rangle$	$\sqrt{B_{\rm norm}(E2)}/\langle\|\rangle$[a]	Dev. of poly.	$B_{\rm 2band}$	Dev. of 2 band
$8_\gamma \to 8_g$	0	0.6070	0.4228[b] (29)	1.2%	0.06407	−2.7%
$8_\gamma \to 6_g$	−30	0.2970	0.2074 (18)	−0.1%	0.002660	−29.9%
$7_\gamma \to 8_g$	16	0.4472	0.5531 (32)	0.9%	0.06185	1.1%
$7_\gamma \to 6_g$	−14	0.5477	0.3038 (8)	0.5%	0.02829	2.2%
$6_\gamma \to 8_g$	30	0.1961	0.6181(115)	0.5%	0.01697	15.5%
$6_\gamma \to 6_g$	0	0.6030	0.4344[c](12)	−1.6%	0.06494	−5.3%
$6_\gamma \to 4_g$	−22	0.3129	0.2477(4)	−0.1%	0.005628	−6.3%
$5_\gamma \to 6_g$	12	0.4264	0.5303(18)	−0.2%	0.05020	−1.8%
$5_\gamma \to 4_g$	−10	0.5641	0.3392(6)	−0.2%	0.03700	1.1%
$4_\gamma \to 6_g$	22	0.1741	0.6039(67)	−1.8%	0.01117	1.1%
$4_\gamma \to 4_g$	0	0.5922	0.4307[c](23)	−0.7%	0.06330	−2.7%
$4_\gamma \to 2_g$	−14	0.3450	0.3048(24)	0.2%	0.01124	1.6%
$3_\gamma \to 4_g$	8	0.3780	0.4954(29)	0.4%	0.03469	−1.1%
$3_\gamma \to 2_g$	−6	0.5976	0.373(1)	0.2%	0.05018	1.0%
$2_\gamma \to 4_g$	14	0.1195	0.5376(56)	1.2%	0.004212	2.1%
$2_\gamma \to 2_g$	0	0.5345	0.4297[c]	−0.5%	0.05172	−2.0%
$2_\gamma \to 0_g$	−6	0.4472	0.373(2)	0.2%	0.02810	1.0%

[a]The numbers in parentheses are uncertainties from ΔI_γ (cf. Table I) only.
[b]The spread in these $\Delta = 0$ points (i.e., ±1.34%) provides a measure of our uncertainty in the fitted value of $Q_0^\gamma = 8.028\,e$ b. Note that their unweighted average is 0.4294, which is close to the independent $\Delta = 0$ value of 0.4297 for $2_\gamma \to 2_g$.
[c]Note that in Table I the $2_\gamma \to 2_g$ intensity ≡ 1.000; that is, its uncertainty is incorporated into the $2_\gamma \to 0_g$ and $2_\gamma \to 4_g$ intensities.

and the $E2$ parameters and the off-diagonal energy parameter are given by [32]

$$B(E2; 2_g \to 0_g) = \frac{Q_0^2}{16\pi}\cos^2(\gamma + \Gamma), \tag{7}$$

$$B(E2; 2_\gamma \to 0_g) = \frac{Q_0^2}{16\pi}\sin^2(\gamma + \Gamma), \tag{8}$$

$$B(E2; 2_\gamma \to 2_g) = \frac{5Q_0^2}{56\pi}\sin^2(\gamma - 2\Gamma), \tag{9}$$

TABLE IV. Intraband $B(E2)\ e^2\,{\rm b}^2$

Transition	$B_{\rm expt}$[a]	$B_{\rm 2\,band}$	Dev. of $B_{\rm 2\,band}$
$2_g \to 0_g$	1.166	1.166	0.00%
$4_g \to 2_g$	1.686	1.671	−0.9%
$6_g \to 4_g$	1.880	1.852	−1.5%
$8_g \to 6_g$	1.978	1.955	−1.2%
$10_g \to 8_g$	2.011	2.029	0.9%
$12_g \to 10_g$	2.037	2.090	2.6%
$4_\gamma \to 2_\gamma$	0.7636	0.6893	−9.7%
$5_\gamma \to 3_\gamma$	1.224	1.111	−9.2%
$6_\gamma \to 4_\gamma$	1.506	1.351	−10.3%
$7_\gamma \to 5_\gamma$	1.691	1.534	−9.3%
$8_\gamma \to 6_\gamma$	1.818	1.614	−11.22%

[a]Ground intraband from [10] except for $2_g \to 0_g$, which is from [31]. γ intraband from Eq. (1) with $Q_0^\gamma = 8.028\,e$ b.

where

$$\Gamma = -\frac{1}{2}\arctan\left(2\sqrt{3}\frac{G}{F}\right). \tag{10}$$

(In [32]G is related to the axial asymmetry of the inertia tensor.)

From the energies in Table I, the $B(E2)$'s implicit in Table III, and $B(E2; 2_g \to 0_g) = 1.166\,e^2\,{\rm b}^2$ [31], by using Eqs. (5)–(9), we obtained $A = 13.43$ keV, $F = 176.3$ keV, $Q_0 = 7.748\,e$ b, $\gamma = 9.225^\circ$, and $\Gamma = -0.445^\circ$ (whence $G = -0.791$ keV, cf. −0.80 keV, p. 161 [9]). Using these parameters we diagonalized $H(I)$ for $I = 2, 4, 6, 8$ and, from the resulting eigenvectors, obtained $B(E2)$ values. The resulting interband $B(E2)$'s, expressed in the form $\sqrt{B(E2;\ I_i \to I_f)}/\langle I_i 22 - 2|I_f 0\rangle$, could then be compared with the experimental values in Table III. An adjustment of Γ from -0.445° to -0.401° ($G = -0.713$ keV) was found to give the best fit. These values, designated as $B_{\rm 2\,band}$, and their deviations from the experimental values are shown in Table III.

Evidently the cubic term in the Mikhailov plot (cf. the points for the $8_\gamma \to 6_g$ and $6_\gamma \to 8_g$ transitions) has an origin that lies outside of the two-band mixing model space. Further, as shown in Table IV, the intraband $B(E2)$'s for the ground band resulting from this calculation agree well with the experimental values [10]; however, the intraband $B(E2)$'s for the γ band that result are lower than values deduced from Tables III and I (Recall the method described earlier to fit points by a choice of Q_0^γ.) This demonstrates that $Q_0^\gamma \neq Q_0^g$ is not due to a mixing effect.

V. CONCLUSIONS

Intensities of γ-ray transitions in ^{166}Er are determined in this work through high-statistics $\gamma\gamma$ coincidence spectroscopy following the β decay of ^{166m}Ho and ^{166}Tm. These γ-ray intensities, converted to relative $B(E2)$ values, are of sufficient precision that a cubic term is revealed in a Mikhailov plot. Perturbation theory and two-band mixing analysis fail to account for the magnitude of the cubic term.

The results presented here provide a deeper insight into the rotor model applied to nuclei. For the $B(E2)$'s involving lower spin, the rotor description is accurate to $\sim$1%. There is clear evidence that $Q_0^\gamma \neq Q_0^g$ (with a difference of $\sim$5%, where recall $B \sim Q^2$ and so the percent deviation in Q is one-half the percent deviation in B). The higher spin nonlinearities (which appear to rapidly increase for $I = 10$ [22]) are not explained by the descriptions considered here. In conclusion, the present work provides a precise measure of the degree to which the rotor model can describe $E2$ properties of a well-deformed nucleus with $\Delta K = 2$ two-band mixing and it provides an indication of where the description breaks down.

ACKNOWLEDGMENTS

We wish to thank colleagues at the 88-Inch Cyclotron Facility for assistance in the experiments. We thank David Rowe for advice on the perturbation theory approach. This work was supported in part by DOE Grant/Contract Nos. DE-FG02-96ER40958 (Ga Tech), DE-AC03-76SF00098 (LBNL), and DE-FG03-98ER41060 (OSU).

[1] A. Bohr, Mat. Fys. Medd. K. Dan. Vidensk. Selsk. **26** (1952).
[2] D. Ward, P. Colombani, I. Y. Lee, P. A. Butler, R. S. Simon, R. M. Diamond, and F. S. Stephens, Nucl. Phys. **A266**, 194 (1976); M. W. Guidry, P. A. Butler, P. Colombani, I. Y. Lee, D. Ward, R. M. Diamond, E. Eichler, N. R. Johnson, and R. Sturm, *ibid.* **A266**, 228 (1976).
[3] P. O. Lipas, Nucl. Phys. **39**, 468 (1962).
[4] V. M. Mikhailov, Izv. Akad. Nauk SSSR, Ser. Fiz. **28**, 308 (1964) [transl. Bull. Acad. Sci. USSR, Phys. Ser. **28**, 225 (1964)]; **30**, 1334 (1966) [transl. **30**, 1392 (1966)].
[5] B. R. Mottelson, J. Phys. Soc. Jpn. Suppl. **24**, 87 (1968).
[6] L. L. Riedinger, N. R. Johnson, and J. H. Hamilton, Phys. Rev. **179**, 1214 (1969).
[7] C. Y. Wu, D. Cline, E. G. Vogt, W. J. Kernan, T. Czosnyka, A. Kavka, and R. M. Diamond, Phys. Rev. C **40**, R3 (1989).
[8] C. Y. Wu, D. Cline, M. W. Simon, R. Teng, K. Vetter, M. P. Carpenter, R. V. F. Janssens, and I. Wiedenhover, Phys. Rev. C **61**, 021305(R) (2000).
[9] A. Bohr and B. R. Mottelson, *Nuclear Structure*, Vol. 2 (Benjamin, Reading, MA, 1975).
[10] E. N. Shurshikov and N. V. Timofeeva, Nucl. Data Sheets **67**, 45 (1992) (note that there is a decimal point error in the listing of the 305-keV line intensity).
[11] C. Gunther and D. R. Parsignault, Phys. Rev. **153**, 1297 (1967).
[12] C. W. Reich and J. E. Cline, Nucl. Phys. **A159**, 181 (1970).
[13] J. Adam, W. Wagner, W. Zwolska, J. Zwolski, B. Kracik, and M. Fisher, Izv. Akad. Nauk SSSR, Ser. Fiz. **52**, 18 (1988) [transl. Bull. Acad. Sci. USSR, Phys. Ser. **52**, 17 (1988)].
[14] See E. M. O. Bernardes, J. U. Delgado, L. Tauhata, C. J. d. Silva, A. Iwahara, R. Poledna, and A. S. Paschoa, Appl. Radiat. Isotopes **56**, 157 (2002), and references therein.
[15] J. Adam, A. Budziak, W. Wagner, V. Zvolska, I. Zvolski, B. Kracik, and M. Fisher, Izv. Akad. Nauk SSSR, Ser. Fiz. **53**, 875 (1989) [transl. Bull. Acad. Sci. USSR, Phys. Ser. **53**, 53 (1989)].
[16] J. Adam, J. Frána, E. P. Grigoriev, K. Y. Gromov, M. Honusek, T. A. Islamov, and V. O. Sergeev, Czech. J. Phys. B **29**, 997 (1979).
[17] M. Budzynski, E. P. Grigorev, K. Y. Gromov, O. I. Kochetov, G. Lizurei, K. Nezgoda, A. I. Muminov, M. Subotovich, T. Khazratov, and Y. V. Yushkevich, Izv. Akad. Nauk SSSR, Ser. Fiz. **44**, 1831 (1980) [transl. Bull. Acad. Sci. USSR, Phys. Ser. **44**, 42 (1980)].
[18] J. P. Martin, D. C. Radford, M. Beaulieu, P. Taras, D. Ward, H. R. Andrews, G. Ayotte, F. J. Sharp, J. C. Waddington, and O. Hausser, Nucl. Instrum. Methods A **257**, 301 (1987).
[19] R. J. Gehrke, R. G. Helmer, and R. C. Greenwood, Nucl. Instrum. Methods A **147**, 405 (1977).
[20] W. D. Hamilton, H. Marshak, and K. Kumar, J. Phys. G **16**, L219 (1990).
[21] J. Loats, Ph. D. dissertation, Oregon State University, 2004.
[22] C. Fahlander, I. Thorslund, B. Varnestig, A. Bäcklin, L. E. Svensson, D. Disdier, L. Kraus, I. Linck, N. Schulz, and J. Pedersen, Nucl. Phys. **A537**, 183 (1992).
[23] I. Thorslund, C. Fahlander, A. Bäcklin, B. Kotlinski, D. Cline, A. T. Renalds, and E. G. Vogt, Z. Phys. A **342**, 35 (1992).
[24] T. Ichihara, H. Sakaguchi, M. Nakamura, M. Yosoi, M. Ieiri, Y. Takeuchi, H. Togawa, T. Tsutsumi, and S. Kobayashi, Phys. Rev. C **36**, 1754 (1987).
[25] F. K. McGowan, W. T. Milner, R. L. Robinson, P. H. Stelson, and Z. W. Grabowski, Nucl. Phys. **A297**, 51 (1978).
[26] H. J. Wollersheim and T. W. Elze, Z. Phys. A **280**, 277 (1977).
[27] C. Baktash, J. X. Saladin, J. O'Brien, I. Y. Lee, and J. E. Holden, Phys. Rev. C **10**, 2265 (1974).
[28] C. E. J. Bemis, P. H. Stelson, F. K. McGowan, W. T. Milner, J. L. C. J. Ford, R. L. Robinson, and W. Tuttle, Phys. Rev. C **8**, 1934 (1973).
[29] J. M. Domingos, G. D. Symons, and A. C. Douglas, Nucl. Phys. **A180**, 600 (1972).
[30] P. O. Tjøm and B. Elbek, Nucl. Phys. **A107**, 385 (1968).
[31] S. Raman, C. W. Nestor Jr., and P. Tikkanen, At. Data Nucl. Data Tables **78**, 1 (2001).
[32] J. L. Wood, A. M. Oros-Peusquens, R. Zaballa, J. M. Allmond, and W. D. Kulp, Phys. Rev. C **70**, 024308 (2004).